Review

Current Advances in the Carbon Nanotube/Thermotropic Main-Chain Liquid Crystalline Polymer Nanocomposites and Their Blends

Henry Kuo Feng Cheng [1,2], Tanya Basu [1], Nanda Gopal Sahoo [3,*], Lin Li [1] and Siew Hwa Chan [1]

[1] School of Mechanical and Aerospace Engineering, Nanyang Technological University, 50 Nanyang Avenue, 639798, Singapore; E-Mails: kfcheng@simtech.a-star.edu.sg (H.K.F.C.); tbasu@ntu.edu.sg (T.B.); mlli@ntu.edu.sg (L.L.); mshchan@ntu.edu.sg (S.H.C.)

[2] Singapore Institute of Manufacturing Technology, 71 Nanyang Drive, 638075, Singapore

[3] Energy Research Institute, Nanyang Technological University, 50 Nanyang Drive, 637553, Singapore

* Author to whom correspondence should be addressed; E-Mail: ngsahoo@ntu.edu.sg; Tel.: +65-6790-4051; Fax: +65-6791-1859.

Abstract: Because of their extraordinary properties, such as high thermal stability, flame retardant, high chemical resistance and high mechanical strength, thermotropic liquid crystalline polymers (TLCPs) have recently gained more attention while being useful for many applications which require chemical inertness and high strength. Due to the recent advance in nanotechnology, TLCPs are usually compounded with nanoparticles to form particulate composites to enhance their properties, such as barrier properties, electrical properties, mechanical properties and thermal properties. Carbon-based nanofillers such as carbon nanotube (CNT), graphene and graphene oxide are the most common fillers used for the TLCP matrices. In this review, we focus on recent advances in thermotropic main-chain liquid crystalline polymer nanocomposites incorporated with CNTs. However, the biggest challenges in the preparation of CNT/TLCP nanocomposites have been shown to be inherent in the dispersion of CNTs into the TLCP matrix, the alignment and control of CNTs in the TLCP matrix and the load-transfer between the TLCP matrix and CNTs. As a result, this paper reviews recent advances in CNT/TLCP nanocomposites through enhanced dispersion of CNTs in TLCPs as well as their improved interfacial adhesion with the TLCP matrices. Case studies on the important role of chemically modified CNTs in the TLCP/thermoplastic polymer blends are also included.

1. Introduction

Liquid crystalline polymers (LCPs) are considered positionally disordered crystals or orientationally ordered liquids [1,2]. Typically LCPs have several advantages like, outstanding mechanical properties at high temperatures, excellent chemical resistance, inherent flame retardancy and good weatherability [3].

Thermotropic Liquid Crystalline polymers (TLCPs) have been one of the most interesting developments in the chemistry and technology of polymeric materials during the past two decades. TLCPs have gained increased commercial attention because of their unique properties. These include their low coefficients of thermal expansion, low viscosity, high modulus, low permeability to gases, low dielectric constants, and chemical resistance [4,5].

Due to their ease of processing as well as their extraordinary properties compared to many other polymers [6–8], these polymeric materials are able to incorporate with different nano-fillers, such as carbon nanotubes (CNTs), MMT, TiO_2 *etc.*, for the fabrication of polymeric nanocomposites leading to a new area of high performance nanocomposites and fibers due to their unique properties. Besides, TLCPs are currently important commercial materials used to fabricate LCP-based nanocomposites with many applications, which include high-performance composites even used in aerospace application [9–11].

The research and development of CNT/TLCP nanocomposites has greatly increased in recent years for the following reasons. Firstly, the CNT/TLCP nanocomposites showed unpredictable combinations of properties, such as the mechanical and thermal properties, compared to other CNT/polymer nanocomposites. The second reason was related to the discovery of CNTs by Iijima in early 1991 [12]. The unpredictably sophisticated properties of these CNTs, especially their superior mechanical and electrical properties over those of the traditional fillers, offer an exciting potential for new composite materials [13–15].

Moreover, CNTs are found to have unique structural arrangement of atoms, high aspect ratio and excellent mechanical, thermal and electrical properties, making them ideal reinforcing components in host polymer matrices [10]. Additionally, CNTs are highly flexible. This property confers remarkable advantages to CNTs over conventional carbon fibers in composite processing [16]. Thus, researchers have shown great interest in using CNTs for high performance polymer nanocomposites in various applications.

Although there are a number of reviews [17–20] on the physical properties of CNT composites with various polymer matrices, the discussion on the CNT composites with TLCPs is still very limited. This is therefore an appropriate time to study CNT/TLCP composites, not only due to their outstanding combinations of properties which are possible to achieve but also due to their high potential for successful commercial development.

The famous and innovative application of TLCPs is to blend them with other thermoplastics. A polymer blend containing a TLCP and a flexible chain polymer is attractive in two aspects: (1) the TLCP acts as a 'processing aid' to reduce the blend's melt-viscosity [21] and (2) its *in situ* fibrillation

results in a 'self-reinforced' polymeric blend. The morphology and structure of thermoplastic/TLCP blends are highly dependent on their processing conditions [22,23].

On the other hand, TLCPs are immiscible with most thermoplastics at the molecular level due to the thermodynamic instability. This incompatibility between the matrix polymer and dispersed LCP phase leads to poor interfacial adhesion producing a resultant blend with poor mechanical properties. Therefore, the mechanical properties of a TLCP/thermoplastic blend are generally lower than those expected from theoretical calculations. However, a compatibilization with appropriate agent(s) can improve the adhesion between the LCP fibrils and matrix interface. The agents can be referred to as fillers of many kinds such as nanosilica, carbon nanotubes, *etc*.

Recently, TLCP blend systems containing functionalized CNTs have been receiving attention from present researchers. Currently, a number of publications reported that the addition of a small amount of functionalized CNTs into a TLCP/thermoplastic blend could improve its mechanical properties through the enhanced interfacial adhesion between the LCP and the thermoplastic [24]. In this ternary system, the functionalized CNTs act not only as compatibilizers but also as linkages between both phases of the blend. Consequently, the resultant ternary composites show significant improvement in their morphological, mechanical and thermal properties. Therefore, the ternary composite system containing functionalized CNTs, a TLCP and a thermoplastic polymer results in one of the most potential composite systems for aerospace and many other industrial fields.

2. Liquid Crystalline Polymers: The Background

Liquid crystals (LC) are substances that exhibit a phase of matter intermediate to the isotropic liquid and solid crystal states called a mesophase or mesomorphic phase. There are three types of mesophases such as smectic, nematic and cholesteric, which are defined by their type of ordering. Smectic mesophases show ordering in two directions *i.e.*, orientational order and positional order, whereas nematic mesophases show only orientational order. The cholesteric is a subset of the nematic mesophase or more properly the chiral nematic mesophase.

Liquid crystals can be divided into thermotropic and lyotropic LCs. Thermotropic LCs exhibit a phase transition into the LC phase as the temperature is changed, whereas lyotropic LCs exhibit phase transitions as a function of concentration of the mesogen in a solvent (typically water) as well as temperature [25].

LCPs can be classified into two groups, namely the main-chain liquid crystalline polymers and the side-chain liquid crystalline polymers. Each group can be divided into two categories either thermotropic or lyotropic depending on its characteristics. Lyotropic liquid crystalline polymers (LLCPs) exhibit liquid crystallinity in solutions, whereas TLCPs show liquid crystallinity when in the melt [1–3]. Typical TLCPs exhibit superior properties over other thermoplastic polymers due to their unique structure. In this review, we will discuss the thermotropic main-chain liquid crystalline polymers mainly based on Vectra and Rodrun.

3. Challenges for CNTs as Reinforcing Fillers in CNT/liquid Crystalline Polymer Composites

Carbon nanotubes are one-dimensional carbon materials which can have an aspect ratio greater than 1,000. They can be envisioned as cylinders composed of rolled-up graphene planes with diameters in a

nanometre scale [26,27]. There are two main types of carbon nanotubes: single-walled carbon nanotubes (SWCNTs) [28] and multiwalled carbon nanotubes (MWCNTs) [12,29]. The theoretical and experimental results have shown unusual mechanical properties of CNTs. The chemical bonding of an ideal CNT is composed entirely of sp^2 carbon-carbon bonds. This bonding structure, which is stronger than the sp^3 bonds found in diamond, provides CNTs with extremely high mechanical strength [30]. It is well known that the mechanical strength of CNTs exceeds those of any existing materials [30–32]. Typical properties of CNTs are presented in Table 1 [33–36].

Table 1. Typical properties of carbon nanotubes (CNTs) [33–36].

Property	SWCNT	MWCNT
Tensile strength (GPa)	50–500	10–60
Elastic modulus (TPa)	~1	0.3–1
Elongation at break (%)	5.8	-
Density (g/cm^3)	1.3–1.5	1.8–2.0
Electrical conductivity (S/m)	~10^6	
Thermal stability	>700 ℃ (in air)	
Typical diameter	1 nm	~20 nm

SWCNTs = single-walled carbon nanotubes; MWCNTs = multiwalled carbon nanotubes.

Although, the main advantages of adding CNTs into an LCP are enhanced stiffness, modulus and tensile strength as well as improved thermal stability and electrical conductivity, CNTs tend to form stable aggregates or bundles in a polymer matrix due to the very strong van der Waals forces between them [37]. Therefore, they are difficult to separate into individual nanotubes and to disperse homogeneously in an LCP matrix, which thus hampers the mechanical and electrical properties of the fabricated nanocomposites.

Many research efforts have been made in the production of CNT/LCP composites for functional and structural applications. However, even after a number of decades of research, the potential for CNTs as reinforcing fillers has been brutally restricted due to the drawback associated with dispersion of entangled CNTs during the fabrication process and the poor interfacial interaction between CNTs and an LCP matrix. As CNTs are characteristically of small diameter in the nanometre scale with a high aspect ratio and thus an extremely large surface area, their nature of poor dispersion in an LCP matrix is rather different from that of other conventional fillers, such as carbon black and carbon fibers. Therefore, the agglomeration of CNTs in an LCP matrix and the weak interfacial adhesion between CNTs and an LCP matrix can be considered as the main reasons for the reduced mechanical, thermal and electrical properties of their nanocomposites as compared with theoretical predictions based on individual CNTs.
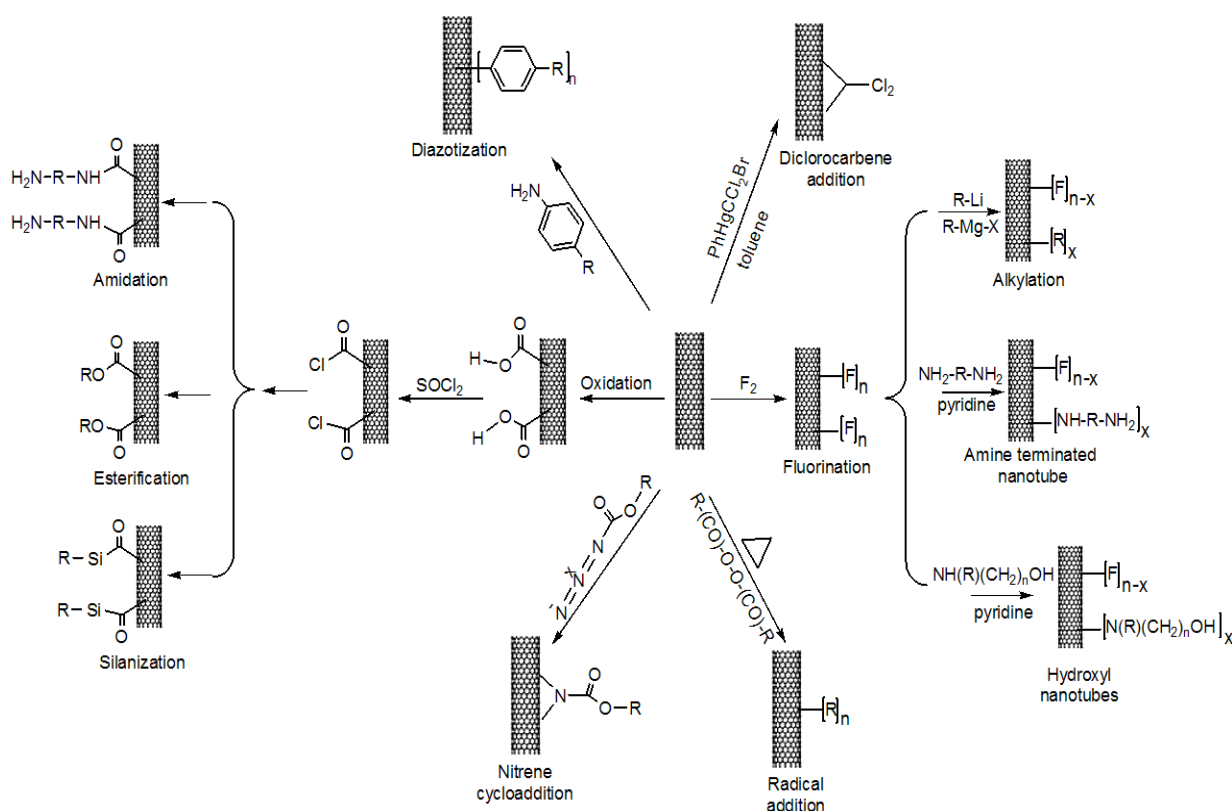
The critical challenges are, therefore, how to incorporate individual CNTs, or at least relatively thin CNT bundles or disentangled CNTs, into a LCP matrix and how to enhance the compatibility as well as the interfacial adhesion between CNTs and an LCP matrix. In addition, the dispersion of CNTs is not only a geometrical problem due to the length and size of the CNTs, but also relates to the method of how to separate individual CNTs from CNT agglomerates and stabilize them in an LCP matrix to avoid the secondary agglomeration [38].

3.1. Modification of Carbon Nanotubes and Their Compatibility with the Liquid Crystalline Polymer Matrix

As mentioned above, the agglomeration of CNTs in an LCP matrix and the poor interfacial adhesion between the CNTs and the LCP molecules are the most critical issues in the fabrication of CNT/LCP composites. Fortunately, several methods are available to improve the dispersion of the CNTs in an LCP matrix as well as to enhance the interaction between the CNTs and the LCP molecules. Particularly, the surface functionalization of CNTs is an effective way to prevent carbon nanotube aggregation by improving the chemical compatibility with the LCP matrixes, which helps CNTs to disperse better and stabilize within an LCP matrix. Moreover, most LCPs contain polar groups, such as esters, benzene rings, ethers *etc*., which are able to react effectively with polar groups of the chemically functionalized CNTs through hydrogen bonding and/or π-π interaction and as a result, the interfacial adhesion between CNTs and LCP molecules is enhanced.

The most common and simple method for the chemical functionalization of CNTs is to introduce carboxylic acid (–COOH) groups on the surface of CNTs. These carboxylic acid groups are usually introduced by oxidation using concentrated sulphuric acid, nitric acid, aqueous hydrogen peroxide, or acid mixture [39]. The acid treated MWCNTs possess some defects on the surface, which are caused by the formation of –COOH groups, while the raw MWCNTs have smooth surfaces because of their perfect lattice structure of carbon-carbon bonds [40–42]. The amount of –COOH groups on the surface of CNTs depends on the oxidation procedure, oxidising agent [43], processing temperature and time [41]. For example, under the same conditions, the concentrations of –COOH groups after treatment with oxidising reagents, H_2SO_4/H_2O_2, NH_4OH/H_2O_2 and HNO_3 are 2.0, 1.6 and 3.8 mmol/g, respectively [43].

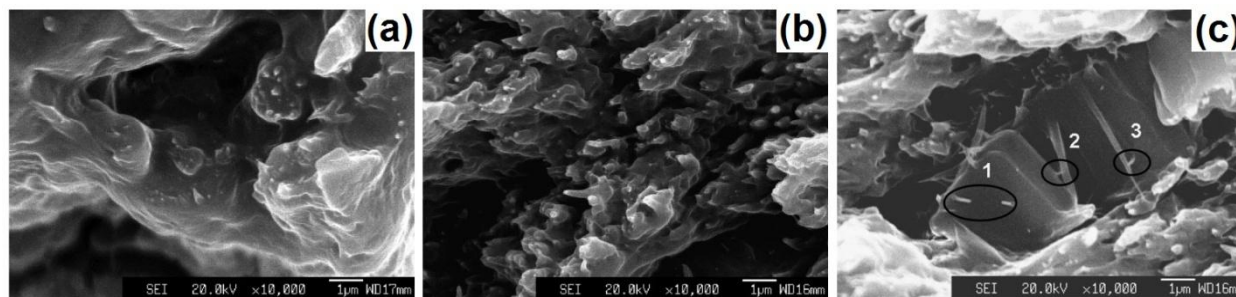**Scheme 1.** Covalent functionalization of carbon nanotubes (CNTs) .

Moreover, the presence of these carboxylic acids can be further employed for covalent attachment of organic or inorganic groups (referring to Scheme 1), leading to highly soluble materials [44]. The sidewalls of the nanotubes could be also functionalised with a fluorination reaction [45]. For example, the fluorinated SWCNTs exhibited improved solubility in isopropanol or dimethyl formamide with ultrasonication [46,47]. Fluorinated CNTs can be further functionalised by alkyl groups using Grignard reagent or alkyllithium compounds that are soluble in chloroform [48]. Direct side-wall functionalisation of CNTs can also be achieved by reactions with carbenes [49], nitrenes [50], radicals [51], *etc.*

In order to study the interfacial adhesion between different chemical groups on the surfaces of CNTs and LCP molecules, our group has recently chemically functionalized MWCNTs with different groups, such as carboxylic acid (–COOH) group [25,52,53], hydroxyl benzoic acid (-HBA) group [53,54], nitrophenyl ($–C_6H_4NO_2$) group [55,56], aminophylnyl ($–C_6H_4NH_2$) group [55], and benzoic acid ($–C_6H_4COOH$) group [55].

4. Dispersion of CNTs in LCP Matrix and Their Interfacial Interaction

In this section, we evaluate the effect of different functionalized MWCNTs on their state of dispersion in a TLCP matrix and their interfacial interaction with the TLCP matrix, as they are the key determiners of the properties of the CNT/TLCP composites. The field emission electron microscope (FESEM) is usually used to study the state of dispersion of CNTs in a polymer matrix.

Figure 1. Field emission electron microscope (FESEM) micrographs for (**a**) raw MWCNT/TLCP, (**b**) MWCNT-COOH/TLCP and (**c**) MWCNT-HBA/TLCP. Reprinted with permission from Reference [53]. Copyright 2009, John Wiley & Sons, Inc.
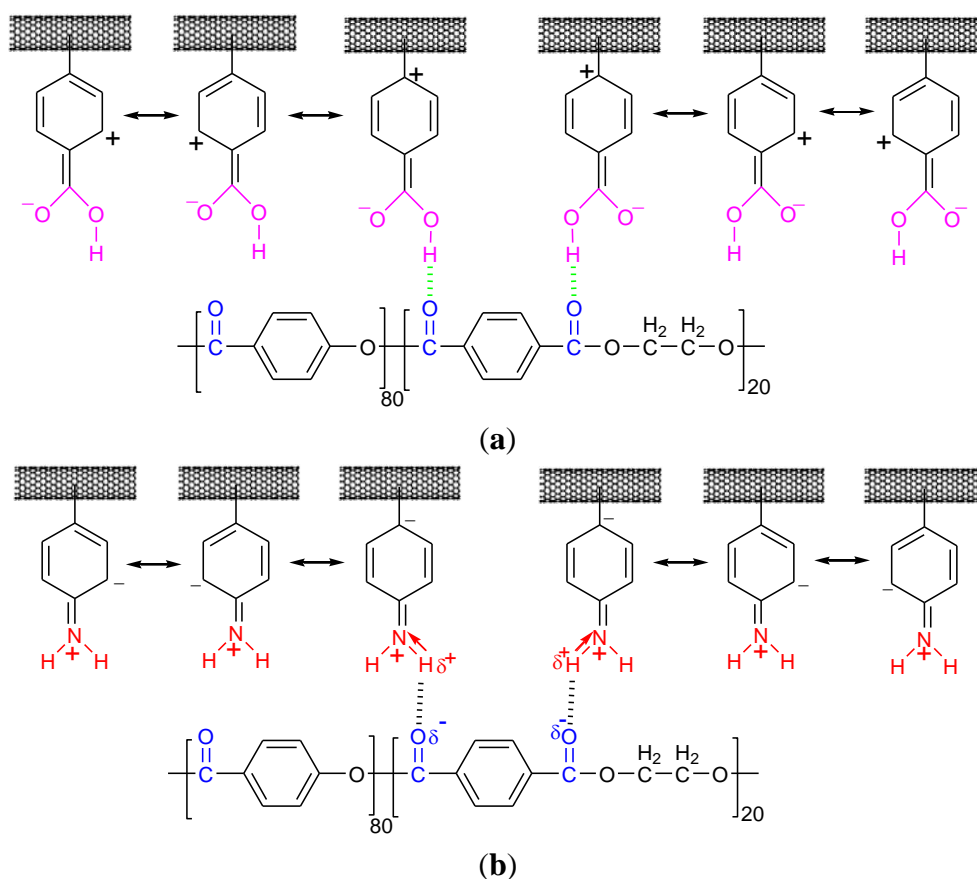

As shown in Figure 1, it is clearly seen that MWCNT-COOH (Figure 1(b)) and MWCNT-HBA (Figure 1(c)) were able to disperse more uniformly than the raw MWCNTs (Figure 1(a)) in the TLCP matrix (Rodrun LC5000). The samples were prepared by a melt mixing using a micro-mixer. Prior to the analysis, the samples were fractured by tensile test and the fractured surfaces of the samples were studied in a field emission electron microscope (FESEM) after gold coating. In Figure 1(a,b), there are well-dispersed bright dots and lines, which represent the end of the broken MWCNTs. Besides, the MWCNTs were broken rather than pulled out from the TLCP matrix and the fibrillation of TLCP matrix was also obviously observed in both cases. This was because the carboxylic (–COOH) groups attached on the MWCNTs provided stronger interaction with the TLCP matrix, probably through H-bonding. In addition, for MWCNT-HBA, the longer chemical moieties containing benzene rings attached on the surface of the MWCNTs imparted an ability to loosen and eventually individualize

bundled nanotubes and then provided strong interactions with the TLCP chains via π-π interaction. Therefore, the strong interaction between the HBA-functionalized MWCNTs and the TLCP matrix greatly enhanced the dispersion as well as the interfacial adhesion.

The variation in H-bonding between the functional groups of MWCNT and a TLCP matrix is also correlated to the properties of the resultant MWCNT/TLCP nanocomposite. In order to study this, we introduced three different chemical groups *i.e.*, $-C_6H_4NO_2$, $-C_6H_4COOH$, and $-C_6H_4NH_2$ to the sidewalls of MWCNTs in order to make MWCNTs more compatible with the LCP [55]. Simultaneously, the effects of electron withdrawing ($-NO_2$ and $-COOH$) and donating ($-NH_2$) groups attached to the benzene rings of the functionalized MWCNTs on the dispersion of MWCNTs in the TLCP matrix and the interaction with the TLCP were investigated. The nature of interaction between the chemical groups on the surface of MWCNTs and TLCP, the shift in absorption wavelength of the $-CO$ groups in the TLCP was analyzed by FTIR.

Scheme 2. Possible formation of hydrogen bonding (**a**) between a thermotropic liquid crystalline polymer (TLCP) chain and MWCNT-C_6H_4COOH and (**b**) between a TLCP chain and MWCNT-$C_6H_4NH_2$ [55]. Reproduced by permission of The Royal Society of Chemistry.

(**a**)

(**b**)
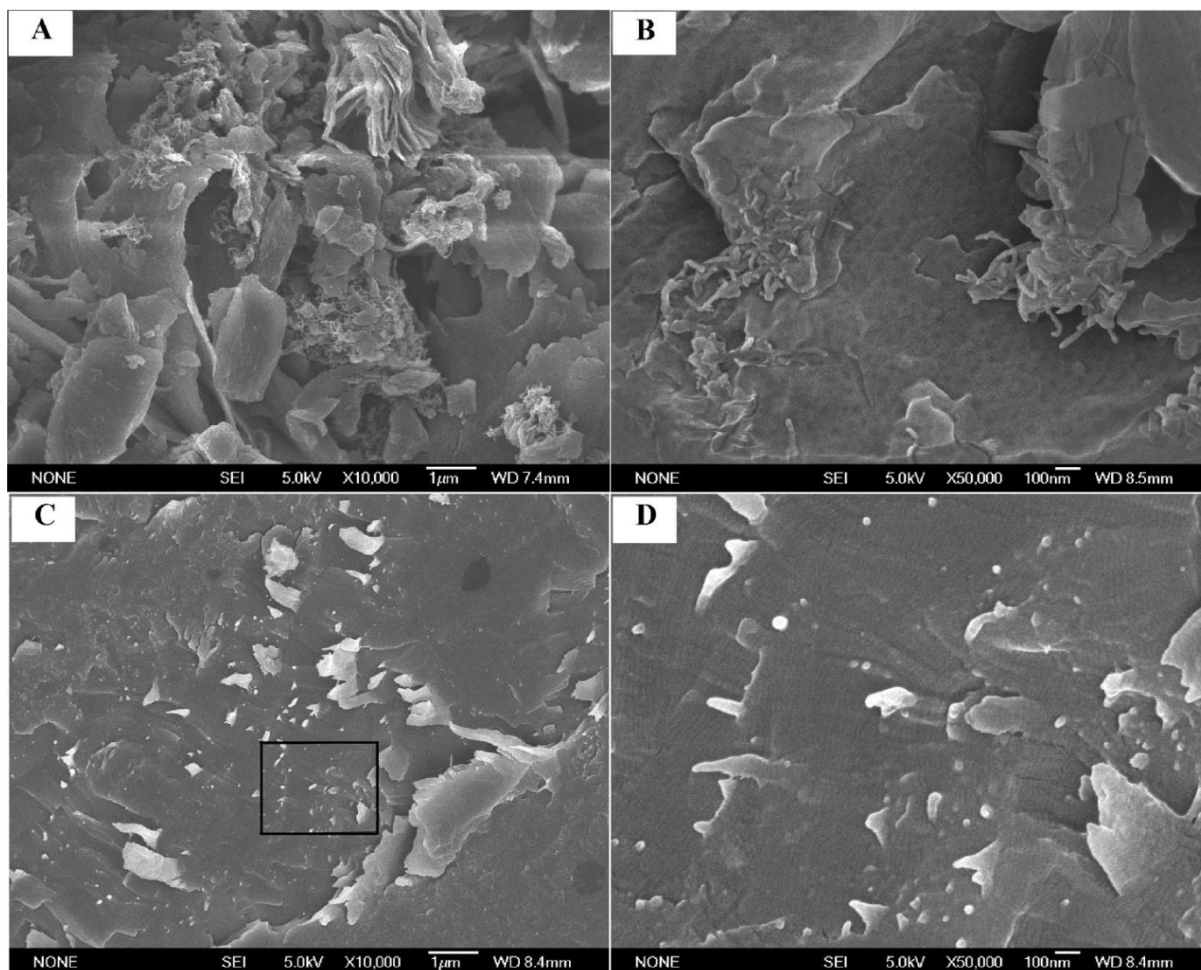
The $-C=O$ peak position was more shifted from 1,720 cm^{-1} in the TLCP to 1,690 cm^{-1} in the nanocomposite with the MWCNT-$C_6H_4NH_2$, suggesting that there is a stronger intermolecular interaction between the MWCNT-$C_6H_4NH_2$ and TLCP than that between the MWCNT-C_6H_4COOH (or MWCNT-$C_6H_4NO_2$ or raw MWCNTs) and TLCP. This is considered to be due to the formation of

hydrogen bonding between the MWCNT-$C_6H_4NH_2$ and the TLCP chains as shown in Scheme 2. The $-C_6H_4NH_2$ functionalized MWCNTs exhibited the highest intermolecular interaction between MWCNTs and TLCP. Due to the electron donating group (-NH_2) attached to the benzene ring, one of the hydrogen atoms of the -NH_2 group had a delta positive charge as in Scheme 2. As a result, there was a possibility of formation of stronger hydrogen bonding between the MWCNT-$C_6H_4NH_2$ and the TLCP matrix. However, this mechanism was not valid in the MWCNT-C_6H_4COOH/TLCP composite.
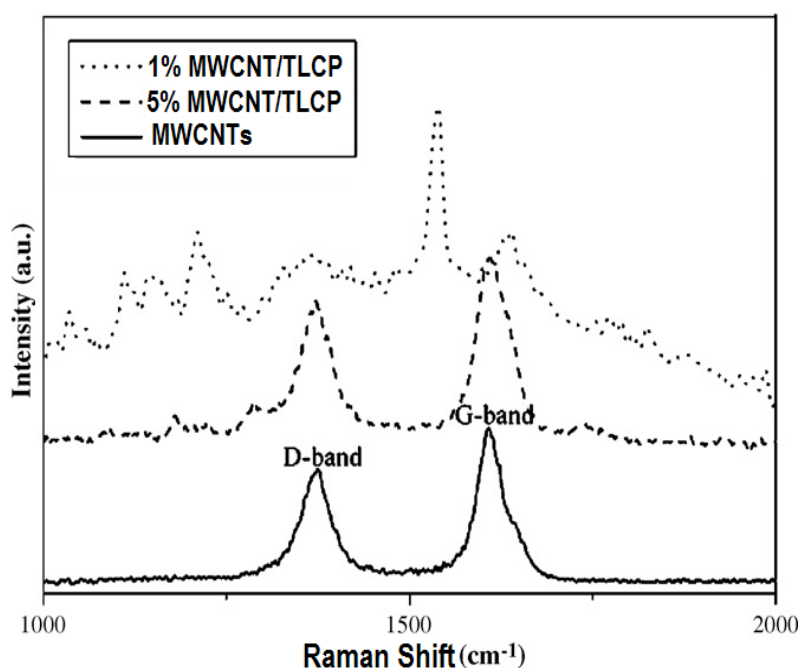
Wu *et al.* [57] fabricated MWCNT/TLCP nanocomposites using the MWCNT-grafted-TLCP (MWCNT-g-LCP). The MWCNTs were firstly functionalized with hydroxyphenyl groups (Ph-OH) and then grafted with the TLCP synthesized from Terephthaloyl Chloride and 1,6-Hexylene Bis(4-hydroxybenzoate) using an *in situ* polycondensation approach. The FESEM images (Figure 2(A,C)) showed that the MWCNT-g-TLCP had a better dispersivity than the purified MWCNTs in the composites. The MWCNT-g-TLCP content in the composite was fixed at 3 wt%. Besides, the fractured surface of the TLCP composite containing MWCNT-g-TLCP displayed a distinct characteristic of ductile fracture (Figure 2(D)). Therefore, it was concluded that the grafting of TLCP onto the MWCNTs could not only improve the dispersion of the MWCNT-g-TLCP but also enhance the toughness of the TLCP matrix in the composites.

Figure 2. FESEM images of (**A**,**B**) MWCNT/TLCP composites with 3 wt.% of purified MWCNTs, (**C**) MWCNT-g-TLCP/TLCP composites containing 3 wt.% of MWCNT-g-TLCP. (**D**) Enlarged morphology of indicated region in C. Reprinted with permission from [57]. Copyright (2011) American Chemical Society.

Wang *et al.* [58] systhesized a polyester-based TLCP via low-temperature solution polycondensation from 1,4-Bis(4-Hydroxybenzoyloxy) butane and terephthaloyl dichloride. Their composites of MWCNT/TLCP were prepared using an *in situ* polymerization method. They used Raman spectroscopy to determine the interaction between the MWCNTs and the TLCP matrix in their composites. Figure 3 shows the Raman spectra of MWCNTs and TLCP/MWCNTs nanocomposites. Two characteristic peaks observed at approximately 1,375 and 1,600 cm^{-1} from the MWNTs curve are usually known as the D-band and the G-band, respectively. The G-band is related to the structural intensity of the sp^2-hybridized carbon atoms of the CNT while the D-band reflects the disorder-induced carbon atoms, resulting from the defects in the carbon nanotube and their ends.

Figure 3. Raman spectra of MWCNTs and MWCNT/TLCP nanocomposites. Reprinted with permission from Reference [58]. Copyright 2010, Elsevier Science Ltd., UK.

It can be seen that the Raman shift of the G-band of 5 wt.% MWCNT/TLCP nanocomposites was clearly increased and the Raman shift of D-band was slightly increased as compared to pure MWCNTs. Besides, even though the relative intensity of the G-band and D-band of 1 wt.% MWCNT/TLCP had reduced, its Raman shifts towards the higher numbers were still observed. The Raman shifts of the D-band and G-band of 1 wt% MWCNT/TLCP composite were more obvious than those of the 5 wt.% MWCNT/TLCP composites, which proved the interactions between TLCP and MWNTs decreased when employing high MWCNTs loadings. It was suggested that the Raman shifts of the D-band and G-band in the MWCNT/TLCP composite could be associated with π-stacking interactions at the surfaces of MWCNTs, involving the aromatic core structure of the TLCP molecules, affecting the vibrational modes of MWCNTs. In particular, the radial breathing mode band, related to vibrations perpendicular to the long axis of the tube, can be affected by extraneous molecules adsorbing onto the nanotube surface. This band acts thus as a sensitive probe for studying the interactions between the MWCNTs and the TLCP host molecules. The existence of strong binding interaction between

MWCNT and TLCP through π-stacking was also reported by Lebovka *et al.* using Fourier transformation infrared spectroscopy [59].

To summarize, the homogeneous dispersion of MWCNTs in an LCP matrix and their improved interfacial adhesion with the LCP matrix can be achieved by a proper selection of chemical groups attached onto the sidewalls of the MWCNTs.

5. Physical Properties of CNT/LCP Nanocomposites

5.1. Rheological Properties of MWCNT/TLCP Nanocomposites

The study of the rheological properties is very important for a nanocomposite. This is because the rheological properties of a nanocomposite are closely related to the state of dispersion and the orientation of the nanofillers in the matrix as well as the interactions between the fillers and the matrix [60].

From Figure 4, it is clearly seen that the TLCP (Rodrun LC5000) and the MWCNT/TLCP nanocomposites exhibited non-Newtonian and shear thinning behaviors over the frequency range studied [55]. It is also observed from Figure 4a that the raw MWCNT/TLCP nanocomposite and the functionalized MWCNT/TLCP nanocomposites are higher in viscosity than the neat TLCP over the frequency studied, showing the common effect of solid fillers on viscosity. However, it is interesting to note that the addition of 1 wt.% of MWCNT-C_6H_4COOH to TLCP could largely increase the viscosity, especially at low frequencies, showing that the interconnected or network-like structures were formed in this nanocomposite due to the CNT-CNT or CNT-TLCP interactions. Moreover, it is interestingly to note that the -$C_6H_4NH_2$ functionalized MWCNTs exhibited the most pronounced effect on melt viscosity among the MWCNT/TLCP nanocomposites studied. Figure 4(a) indicates that the –$C_6H_4NH_2$ functionalized MWCNTs have the strongest interaction with the TLCP, followed by MWCNT-C_6H_4COOH, MWCNT-$C_6H_4NO_2$, and raw MWCNTs.

Figure 4(b,c) shows the storage modulus (G') and loss modulus (G'') of the TLCP and MWCNT/TLCP composites as a function of angular frequency. From these figures, it can be seen that the TLCP and MWCNT/TLCP composites had a non-Newtonian behavior. This non-terminal behavior or secondary plateau might be attributed to the formation of nanotube networks, which could restrict the long-range motion of polymer chains.

The rheological properties of MWCNT/TLCP nanocomposites with different functionalized MWCNTs are listed in Table 2. From this table, it can be clearly concluded that the power law indices for complex viscosity (η*) of the TLCP nanocomposites with the functionalized MWCNTs were always higher than those of the neat TLCP or the TLCP nanocomposites with the raw MWCNTs. This revealed that there was a stronger interfacial interaction between the functionalized MWCNTs and the TLCP matrix. Moreover, the power law indices for storage modulus (G') of the TLCP nanocomposites with the functionalized MWCNTs were closer to zero which suggested that the storage modulus of the MWCNT/TLCP nanocomposites were frequency-independent at the lower frequencies due to the formation of a MWCNT network in the LCP matrix.

Figure 4. (**a**) Complex viscosity (η*) versus angular frequency (ω), (**b**) storage modulus (G') versus angular frequency (ω), and (**c**) loss modulus (G") versus angular frequency (ω) for MWCNT/TLCP composites at 300 ℃ [55]. Reproduced by permission of The Royal Society of Chemistry.
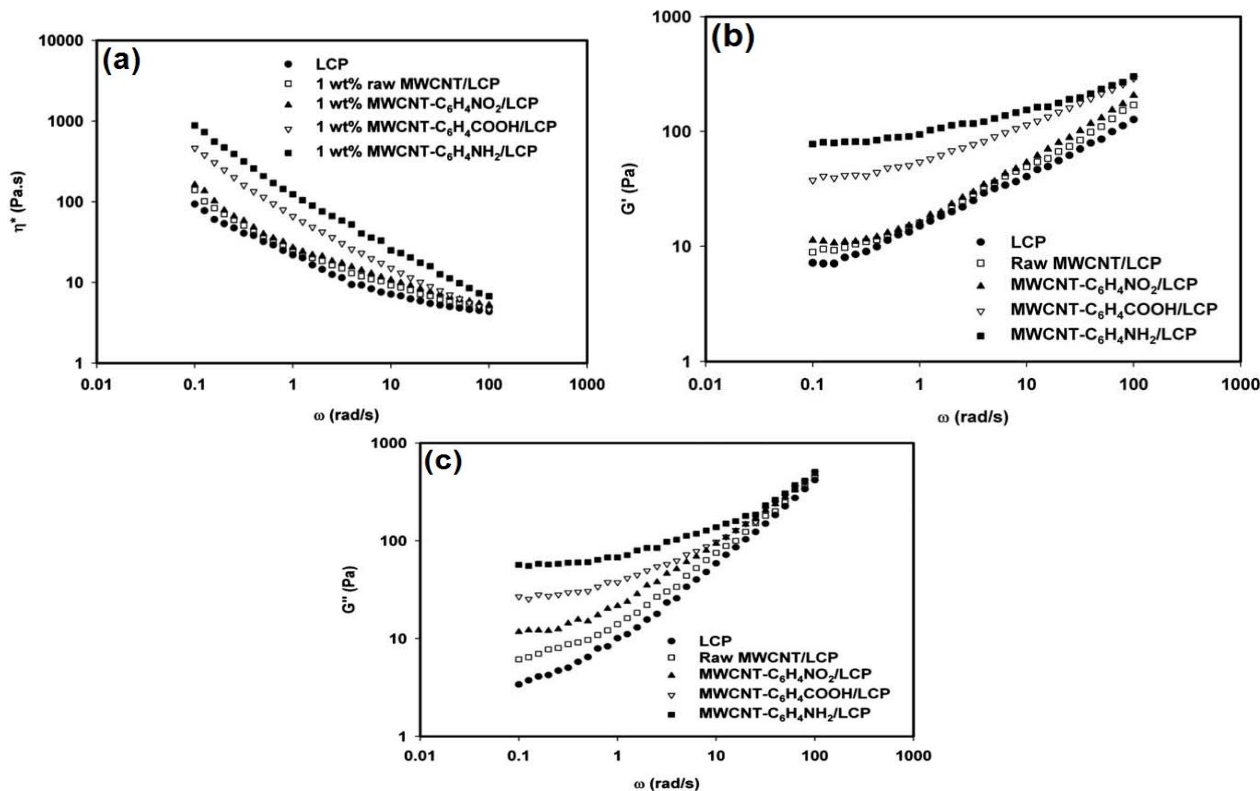

Table 2. Power law indices for complex viscosity (η*), storage modulus (G'), and loss modulus (G") with respect to angular frequency (ω) where the amount of MWCNT was fixed at 1 wt.%.

Sample	log η* *vs.* log ω	log G' *vs.* log ω	log G" *vs.* log ω	References
LCP	0.64 ~ 0.66	0.201 ~ 0.38	0.280 ~ 0.46	[54–56]
Raw MWCNT/TLCP	0.71 ~ 0.82	0.147 ~ 0.25	0.102 ~ 0.34	[54–56]
MWCNT-COOH/TLCP	0.84	0.122	0.098	[54]
MWCNT-HBA/TLCP	0.88	0.116	0.088	[54]
MWCNT-C_6H_4COOH/TLCP	0.84	0.14	0.16	[55]
MWCNT-$C_6H_4NO_2$/TLCP	0.78	0.18	0.27	[55,56]
MWCNT-$C_6H_4NH_2$/TLCP	0.88	0.07	0.08	[55]

5.2. Electrical Properties of MWCNT/TLCP Nanocomposites

As CNTs exhibit high aspect ratio and high electrical conductivity, they are excellent candidates for fabrication of electrically conducting nanocomposites. While the electrical conductivity of individual carbon nanotubes has been measured to be in the order of 10^6 S/m [61], the maximum electrical conductivity of SWCNT films has been reported to be in the range of 10^4 to 10^5 S/m [62,63] due to the contact resistance between the individual carbon nanotubes in the films. Therefore, the range of electrical conductivity of CNT/polymer composites as reported is tremendously wide. Again, the

electrical conductivity of CNT/polymer composites is widely defined by percolation theory. The percolation threshold of CNT/polymer composites has been reported to range from 0.0025 vol.% [64] to several vol.%. [65]. The key factors determining a percolation threshold for electrical conductivity in CNT/polymer nanocomposites include dispersion [66], alignment [67], and aspect ratio [66–68] of carbon nanotubes [66]. Besides, the electrical conductivity of CNT/polymer nanocomposites closely depends on the processing method and the type of functionalization of CNTs [69,70]. Therefore, it is difficult to draw definite conclusions about the mechanism of electrical conductivity of CNT/polymer composites from the literature. This is because the reported levels of CNT loading to achieve a percolation threshold vary widely.

Recently we have studied the electrical conductivity of the TLCP (Rodrun LC 5000) nanocomposites with raw and different functionalized MWCNTs fabricated by a melt-mixing technique [52,53]. The electrical conductivities of the MWCNT/LCP nanocomposites are listed in Table 3.

Table 3. Electrical conductivity of the MWCNT/TLCP nanocomposites.

Sample	MWCNT (wt.%)	Electrical Conductivity (S/cm)	References
TLCP	1	1.33×10^{-13}	[55,56]
Raw MWCNT/TLCP	1	9.80×10^{-12}	[55,56]
MWCNT-C_6H_4COOH/TLCP	1	2.75×10^{-11}	[55]
MWCNT-$C_6H_4NH_2$/TLCP	1	4.38×10^{-11}	[55]
MWCNT-$C_6H_4NO_2$/TLCP	1	1.13×10^{-11}	[55,56]

From Table 3, it is seen that the electrical conductivity of the LCP increased about 10 times when incorporated with 1 wt.% of raw MWCNT. Moreover, the electrical conductivities of the TLCP nanocomposites with the functionalized MWCNTs were much higher than that of the raw MWCNT/TLCP nanocomposite at 1 wt.% MWCNT loading. This is because the functionalized MWCNTs were able to disperse well in the TLCP matrix to form electrical pathways due to their improved compatibility with the TLCP. Additionally, the improvement in the dispersion of MWCNTs in the polymer matrix by their surface functionalization could lead to improvement in the electrical properties by helping them to form an electrically conductive network throughout the matrix [71,72]. Among these, the MWCNT-$C_6H_4NH_2$/TLCP nanocomposites showed the highest electrical conductivity of 4.38×10^{-11} S/cm at 1 wt.% MWCNT loading. The higher extent of H-bonding between the MWCNT-$C_6H_4NH_2$ and the TLCP matrix is probably the reason that the MWCNT-$C_6H_4NH_2$/TLCP nanocomposites possessed the highest electrical conductivity among the composites studied. Apart from the functionalization of MWCNTs, the content of MWCNTs in the TLCP matrix also played an important role for the improvement in electrical conductivity of the MWCNT/TLCP nanocomposites.

However, the electrical conductivities of the MWCNT/TLCP composites with both raw MWCNTs and functionalized MWCNTs were lower than those of the theoretical perditions. This is because for the composites with the raw MWCNTs, the dispersion state of MWCNTs in the TLCP matrix was not within the satisfactory level. However, for the composites with the functionalized MWCNTs, the flawless electronic structure of MWCNT was destroyed during the functionalization. Due to the severe environment during the functionalization, the sp^2 carbon structure of MWCNTs was changed to sp^3 carbon structure during the covalent functionalization and thus, their excellent electronic structure was

demolished [65,66]. Therefore, to improve the electrical properties of MWCNT/polymer composites, a balance is required between the improved dispersion of MWCNTs in the matrix and the damage to their carbon-carbon bonds due to the covalent functionalization.

5.3. Mechanical Properties of MWCNT/TLCP Nanocomposites

Thermotropic liquid crystalline polymers (TLCPs) are composed of long chain rigid rod-like molecules that exhibit an ordered structure in the melt. Therefore, TLCPs have attracted considerable attention for researchers because of their high mechanical strength and modulus, excellent dimensional stability, as well as good processability [13,73]. The mechanical properties for different MWCNT/TLCP composites are summarized in Table 4.

For example, Park *et al.* [14] prepared the TLCP nanocomposites reinforced with carboxylated MWCNTs through melt compounding in a twin screw extruder. In this study, the amount of carboxylated MWCNT incorporated into the LCP was lowered to 0.01–0.2 wt.%. Incorporation of these very small amounts of carboxylated MWCNTs improved the mechanical properties of MWCNT/LCP nanocomposites, and this was attributed to the reinforcement effect of carboxylated MWCNTs with a high aspect ratio and their uniform dispersion in the LCP matrix.

Table 4. Mechanical Properties of MWCNT/TLCP composites.

Functionalization ofMWCNT	MWCNT Loading (wt.%)	Improvement in Modulus (%)	Improvement in tensile strength (%)	References
Oxidized	1.5	34.1	41.4	[72]
Pristine	1	6	28	[53]
Hydroxybenzoic acid	1	41	55	[53]
Hydroxybenzoic acid	4	66	90	[54]
Nitrophenyl	4	43	80	[56]
Aminophylnyl ($C_6H_4NH_2$)	1	38	50	[55]
Pristine	2	43	60	[74]

Kim *et al.* [15] fabricated the nanocomposites based on TLCP, synthesized from poly(p-hydroxybenzoate) and poly(ethylene terephthalate) with a molar ratio of 80:20 and a very small quantity of MWCNTs by direct melt compounding in a twin-screw extruder. The tensile strength and modulus of a composite containing 1.5 wt.% of MWCNT-COOH were enhanced by 41.4% and 34.1%, respectively as compared to its respective pure LCP.

Choi *et al.* reported that the tensile strength and modulus of MWCNT/TLCP nanocomposites increased from 62.3 in pure LTCP to 89.3 MPa (an increase of 43.3%) and 1.12 to 1.79 GPa (an increase of 59.8%), respectively, when the MWCNTs content reached 2 wt.% in CNT/LCP nanocomposites [75].

Our group has been working on the preparation of high performance polymer composites from MWCNTs and a TLCP (Rodrun LC5000) [53–56]. We have a novel approach to chemical functionalization of MWCNTs for fabricating advanced polymeric nanocomposites with TLCP [53]. In our approach, two types of chemical moieties (*i.e.*, carboxylic and hydroxyl benzoic acid groups) are selectively introduced onto the sidewalls of the MWCNTs. The TLCP used is composed of 80%

4-hydroxybenzoic acid (HBA) and 20% ethylene terephthalate (ET). Because HBA is the predominant component of the TLCP, we expected that in the TLCP matrix the dispersion of the HBA-grafted MWCNTs would be better than that of pristine MWCNTs.

The tensile strength and modulus of the nanocomposite with 1 wt.% raw MWCNTs were enhanced by 6% and 28%, respectively, as compared to the pure LCP. As expected, HBA groups on the MWCNTs contributed to the significant enhancement in the tensile strength and modulus by 41% and 55%, respectively.

In addition, for the theoretical prediction of the modulus of randomly distributed filler-reinforced nanocomposites, the Halpin–Tsai model [75–78] is widely used in many literature references. For the moduli of randomly oriented MWCNTs in the TLCP matrix, the Halpin–Tsai model proposed $E_{composite}$ which is governed by the following set of equations.

$$E_{composite} = E_{TLCP} \left[\frac{3}{8} \frac{1+2(L_{MWCNT}/D_{MWCNT})(\eta_L V_{MWCNT})}{1-(\eta_L V_{MWCNT})} + \frac{5}{8} \frac{1+(2\eta_T V_{MWCNT})}{1-(\eta_T V_{MWCNT})} \right] \qquad (1)$$

$$\eta_L = \frac{(E_{MWCNT}/E_{TLCP})-1}{(E_{MWCNT}/E_{TLCP})+2(L_{MWCNT}/D_{MWCNT})}, \eta_T = \frac{(E_{MWCNT}/E_{TLCP})-1}{(E_{MWCNT}/E_{TLCP})+2} \qquad (2)$$
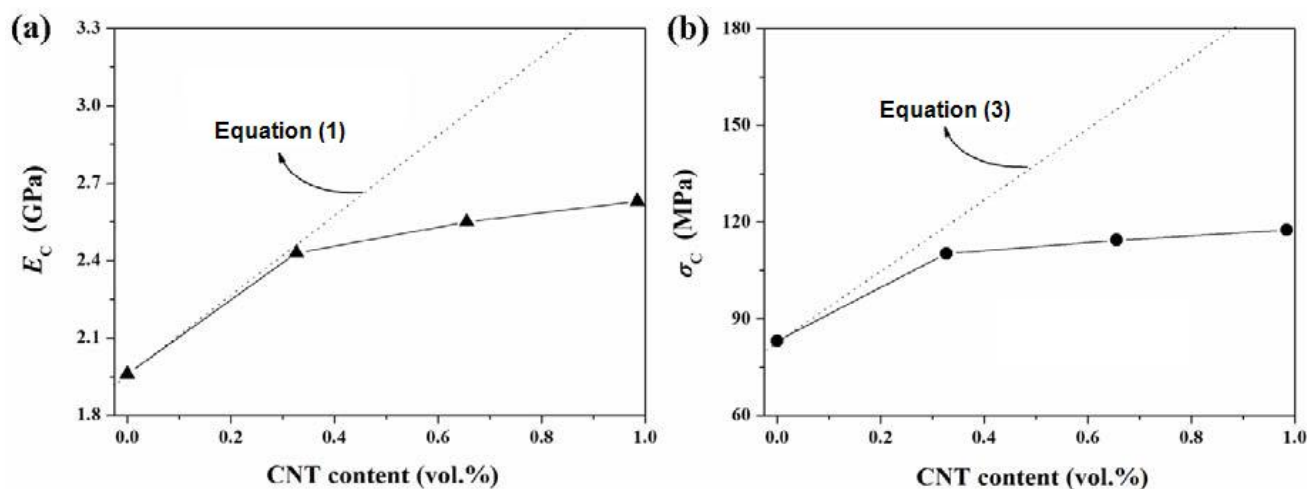
where $E_{composite}$ represents the Young's modulus of the nanocomposite with randomly distributed MWCNTs. E_{MWCNT} and E_{TLCP} are Young's moduli of the MWCNTs and the TLCP matrix, respectively. L_{MWCNT}, and D_{MWCNT} refer to the length and diameter of the MWCNT, and V_{MWCNT} is the volume fraction of MWCNTs in the nanocomposites. The theoretical tensile strength of MWCNT/TLCP composites can be determine from the following equation: [79]

$$\sigma_{composite} = \sigma_{MWCNT} V_{MWCNT} + \sigma_{TLCP} V_{TLCP} \qquad (3)$$

where $\sigma_{composite}$, σ_{MWCNT}, and σ_{TLCP} are the tensile strength of the MWCNT/TLCP composites, MWCNT and TLCP, respectively.

Kim *et al.* [80] used the Halpin–Tsai model to compare their experimental result to the theoretical ones. The L_{MWCNT}/D_{MWCNT} (aspect ratio) was taken as 1,000. The Young's modulus of MWCNTs was 450 GPa. The density of the TLCP matrix was taken as 1.41 g/cm^3, and that of the MWCNT was 2.16 g/cm^3. The theoretically predicted value of σ_{MWCNT} was considered as 11 GPa. As shown in Figure 5, the experimental results for mechanical properties of TLCP nanocomposites were lower than the theoretically predicted values. This result was explained by the curvature of MWCNTs in TLCP nanocomposites: some MWCNTs embedded in a TLCP matrix often exhibit curved morphology, and not a straight one. This curvature feature of MWCNT in TLCP matrix also has the possibility to decrease the nanoreinforcing effect of MWCNT in TLCP composites, in comparison with the theoretical reinforcement provided by straight inclusions. Therefore, the nanoreinforcing effect of CNT would be more effective in improving the mechanical properties of TLCP nanocomposites when the introduced CNT exhibits straight morphology within the TLCP matrix and it is preferentially aligned along its axial direction.

Figure 5. Comparison between the theoretical predictions (dotted line) and the experimental results (solid line) of the modulus (**a**) and of the tensile strength (**b**) for the MWCNT/TLCP composites [80].

Therefore, we can draw the conclusion that the overall improvement in the mechanical properties of TLCP nanocomposites is expected to be further improved by optimizing the unique geometric feature and alignment of the CNT in the TLCP matrix as well as the combination of the enhanced interfacial adhesion between the CNT and the TLCP matrix with good dispersion of the CNT in the TLCP matrix during the melt processing.

6. TLCP Blends and Their Nanocomposites

TLCPs are usually added to other polymers in order to reduce their melt viscosity as well as to improve their processability. On the other hand, most of the thermoplastics are generally immiscible with TLCP at a molecular level [81,82]. Moreover, this immiscibility also makes the blend thermodynamically less stable due to weaker interfacial adhesion and as a result, the blend has poor mechanical properties compared to the matrix polymer and the TLCP. Fortunately, if the chemically modified MWCNTs behave like bonding agents or a compatibilizers present at the interface between the TLCP and the matrix polymer, then the MWCNTs will possess an additional function over the reinforcing function of fillers. Besides, the compatibilization effect of the chemically modified CNTs can enhance the fibrillation of TLCP in the composites which can significantly increase the mechanical properties of the composites [83–85].

In other words, as most TLCPs have electronegative groups (such as C=O), the polar groups (–COOH) on the carboxylic modified MWCNTs could show attractive forces to electronegative groups (such as oxygen atoms) in the TLCP chains. Moreover, the -COOH groups of the MWCNT-COOH are also compatible with some of the polar polymers such as nylon. As a result, the chemically modified MWCNTs have the possibility to act as compatibilizers at the interface between the TLCP and nylon [83].
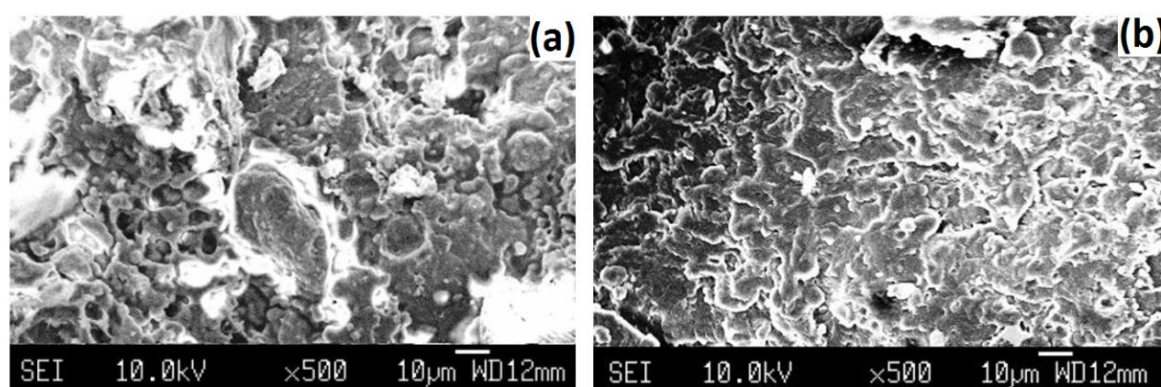
Recently, our group reported in a number of publications [83–85] that the functionalized MWCNTs acted not only as reinforcement fillers but also as compatibilizers that could enhance the interfacial adhesion between TLCP and thermoplastics. We added the carboxylic acid modified multiwalled

carbon nanotubes (MWCNT-COOH) into the different LCP/polymer blends such as, TLCP (Vectra A950)/polyetherimide (PEI), TLCP (Rodrun LC5000)/nylon 6 (PA6) and TLCP (Vectra A950)/poly(ether ether ketone) (PEEK: Victrex 380G). Then, the compatibilizing effect of MWCNT-COOH on the different TLCP/polymer blends was reported in detail. The compatibilizing effect of MWCNT-COOH on the mechanical properties of different TLCP/polymer blends is listed in Table 5. From this table, it was shown that with an addition of a small amount of MWCNT-COOH into the TLCP/polymer blends, their modulus and tensile strength were enhanced more significantly compared to that of raw MWCNTs.

Table 5. Enhancement of the mechanical properties of TLCP/polymer blend with and without incorporating raw and functionalized MWCNTs.

Sample (wt.%) [R-MWCNT and F-MWCNT are raw and functionalized MWCNT, respectively]	MWCNT content (wt.%)	Young Modulus (MPa)		Tensile Strength (MPa)		References
		Young Modulus	% increase to matrix	Tensile Strength	% increase to matrix	
LCP/PA6 (20/80)	0	428.5	-	24.9	-	[25,83]
F-MWCNT/LCP/PA6	1	693	61.7	35.9	44.2	
LCP/PEEK (37.5/62.5)	0	7,100	-	101	-	
R-MWCNT/LCP/PEEK	0.6	9,200	29.6	119	17.8	[84]
F-MWCNT/LCP/PEEK	0.6	10,400	46.5	131	29.7	
LCP/PEI (37.5/62.5)	0	-	-	78	-	
R-MWCNT/LCP/PEI	0.6	-	-	102	30.8	[85]
F-MWCNT/LCP/PEI	0.6	-	-	112.5	44.2	

Figure 6. SEM images of (**a**) TLCP/PA6 blend and (**b**) 1 wt.% MWCNT-COOH/TLCP/PA6 nanocomposite. Reprinted with permission from Reference [24]. Copyright 2010, Trans Tech Publications, Switzerland.

We explained this compatibilizing effect of MWCNT-COOH on the TLCP/PA6 blend by comparing the SEM images of the blend and the MWCNT-COOH composite of the blend [24]. The TLCP phase can be seen as globular domains in the PA6 matrix as shown in Figure 6(a). In Figure 6(a), the blend has many large voids, where the TLCP globules were pulled out from the PA6 matrix, indicating poor interfacial adhesion between the PA6 and TLCP phases. This phenomenon was also observed in the other polymer blends with different TLCPs [84–87]. However, Figure 6(b) shows that there was a

difference in morphology of the composites by adding MWCNT-COOH into the TLCP/PA6 blend. After the addition of 1 wt.% MWCNT-COOH into the TLCP/PA6 blend, a new interesting morphology is observed in Figure 6(b) instead of voids and globules: *i.e.*, TLCP microfibrils appeared, which indicated a better miscibility and strong interfacial adhesion between PA6 and TLCP, in the presence of MWCNT-COOH, which contributes to superior mechanical properties.

Moreover, we proposed a possible mechanism of how the modified MWCNTs perform as a compatibilizer across the interface between PA6 and TLCP to improve the interfacial adhesion between PA6 and TLCP as follows. The functionalized MWCNTs prepared by the acid treatment contain –COOH groups so they are polar. The polar –COOH groups on MWCNTs show attractive forces to electronegative groups (such as oxygen and nitrogen atoms) in the PA6 and TLCP chains. Thus, the MWCNT-COOH could act as a linkage connecting PA6 with TLCP through the formation of hydrogen bonds. As a result of this mechanism, (i) the dispersion of TLCP in the PA6 matrix was enhanced; (ii) the dispersion of MWCNTs in the TLCP/PA6 blend matrix could be improved; and (iii) the overall performance of the composites became much better than using unmodified MWCNTs [83].

7. Applications

LCPs can be considered as an engineering plastic due to their high strength, good chemical resistance, high thermal stability and good heat resistance. However, they are relatively expensive compared to other commodity polymers. Because of their various properties, LCPs are useful for electrical and mechanical parts, food containers, and any other applications requiring chemical inertness and high strength. Therefore, LCPs are traditionally used in engineering applications such as metal replacement for automotives, electronic products, aircraft interiors, bullet-proof body armor, firefighter clothing *etc*.

Fortunately, CNT/TLCP nanocomposties have recently shown many potential applications such as structural components for aircraft bodies, wind turbine blades, light-weight materials for electromagnetic interference (EMI) shielding and materials for strong and flexible fibers. CNT/TLCP nanocomposites are particularly attractive for microwave frequency electronics due to their low relative dielectric constants, low dissipation factors, and the commercial availability of laminates. Packaging microelectromechanical systems (MEMS) is another area where CNT/TLCP nanocomposites have recently gained more attention.

The possibility of obtaining high-strength fibers from liquid crystalline polymers was discovered for the first time in 1965 with the example of an anisotropic solution of poly-p-benzamide (PBA) in an organic solvent of the amide type. Following this, high strength fibers of the Kevlar, Tvaron, and Terlon types have been widely used primarily in techniques for reinforcing tires and other technical rubber articles, such as conveyor belts, hoses, flexible pipes, as well as for creating light composite materials in the aviation industry [88]. In addition, they are also used in the manufacture of cables, ropes, and chords, creating soft protective armor (bullet-proof helmets and vests) and protective clothing and equipment.

Much research effort has been made on the production of MWCNT/TLCP composites for functional and structural applications. However, even after a number of decades of research, the potential for CNTs as reinforcing fillers has been brutally restricted due to the drawback associated with dispersion

of entangled CNTs during the fabrication process and poor interfacial interaction between CNTs and an LCP matrix. Therefore, the application of MWCNT/TLCP composites for functional and structural applications is still relatively narrow.

Jou *et al.* [89] studied high electromagnetic (EM) wave shielding effectiveness (SE) and high mechanical properties of CNT/LCP nanocomposites. They reported that the highest SE for the CNT/TLCP composite obtained was > 62 dB. And the shielding effectiveness of the CNT/TLCP composite strongly depended on the orientation, the aspect ratio and the weight percentage of CNT in the composite.

Chiu *et al.* [90] reported the possibility of a CNT/TLCP nanocomposite as a plastic transceiver module. The shielding effectiveness of their CNT/TLCP composites was suitable for packaging low-cost and high-performance electromagnetic susceptibility (EMS) optical transceiver modules in fiber for home light-wave transmission systems.

8. Concluding Remarks

In this review, we have discussed TLCP nanocomposites incorporated with carbon nanotube (CNTs). The main challenges in the research of CNT/TLCP nanocomposites have been shown to be the agglomeration of CNTs into the TLCP matrix, and the interfacial adhesion between TLCP and CNTs. The functionalization of CNTs could be considered a straight forward and effective way to overcome these issues. However, the selection of the type of functional group which could be attached on the surface of CNTs is the state of art for researchers working in this area. Moreover, the historically well-known problem of the immisciblity between the TLCP and other polymers can be minimized by adding functionalized MWCNTs which contain an appropriate functional group on their surfaces. Although there are some limitations in the commercialization of CNT/TLCP nanocomposites, recent advance in the science of CNT/TLCP nanocomposites shows a great potential for their use in everyday applications.

Acknowledgment

References

1. Godovskii, Y.K.; Papkov, V.S. *Liquid-Crystal Polymers*; Plate, N.A., Ed.; Plenum Press: New York, NY, USA, 1992; Chapter 4, p. 125.
2. Smith, G.W. *Advances in Liquid Crystals*; Brown, G.H., Ed.; Academic Press: New York, NY, USA, 1975; Volume 1, Chapter 4, p. 189.
3. Collings, P.J. *Liquid Crystals: Nature's Delicate Phase of Matter*; Princeton University Press: Princeton, NJ, USA, 1990; pp. 149–167.
4. Tjong, S.C. Structure, morphology, mechanical and thermal characteristics of the *in situ* composites based on liquid crystalline polymers and thermoplastics. *Mater. Sci. Eng. R.* **2003**, *41*, 1–60.

5. Donald, A.M.; Windle, A.H. *Liquid Crystalline Polymer*; Cambridge University Press: Cambridge, UK, 1992; pp. 1–10.

6. D'Allest. J.F.; Sixou, P.; Blumstein, A.; Blumstein, R.B. Investigation of the nematic-isotropic biphase in thermotropic main chain polymers. Homogeneity of the pure nematic and isotropic phases. Part I: Microscopy and fractionation. *Mol. Cryst. Liq. Cryst.* **1988**, *157*, 229–251.

7. Noel, C. *Polymeric Liquid Crystals*; Blumstein, A., Ed.; Plenum Press: New York, NY, USA, 1985; Chapter 2, p. 21.

8. Thomas, E.L.; Wood, B.A. Mesophase texture and defects in thermotropic liquid-crystalline polymers. *Faraday Discuss. Chem. Soc.* **1985**, *79*, 229–239.

9. Vyas, R.; Rida, A.; Bhattacharya, S.; Tentzeris M.M. Liquid Crystal Polymer (LCP): The Ultimate Solution for Low-Cost RF Flexible Electronics and Antennas. In *Proceedings of the Polymers in Defence and Aerospace Applications*, Toulouse, France, 18–19 September 2007; Smithers Rapra Technology: Shropshire, UK, 2007; Section 6, p. 21.

10. Chung, T.S.; Calundann, G.W.; East, A.J. Liquid-crystalline polymers and their applications. In *Encyclopaedia of Engineering Materials*; Chermisinoff, N.P., Ed.; Marcel Dekker: New York, NY, USA, 1989; Volume 2, pp. 625–675.

11. Hearle, J.W.S. *High Performance Fibers*; Woodhead Publishing: Philadelphia, PA, USA, 2001; p. 329.

12. Iijima, S. Helical microtubules of graphitic carbon. *Nature* **1991**, *354*, 56–58.

13. Demus, D.; Gray, G.W.; Speiss, H.W.; Goodby, J.W.; Vill, V. *Handbook of Liquid Crystals*; Wiley-VCH: Weinheim, Germany, 1998; p. 515.

14. Park, S.K.; Kim, S.H.; Hwang, J.T. Carboxylated multiwall carbon nanotube-reinforced thermotropic liquid crystalline polymer nancomposites. *J. Appl. Polym. Sci.* **2008**, *109*, 388–396.

15. Kim, J.Y.; Kim, D.K.; Kim, S.H. Effect of modified carbon nanotube on physical properties of thermotropic liquid crystal polyester composites. *Eur. Polym. J.* **2009**, *45*, 316–324.

16. Kaito, A.; Kyotani, M.; Nakayama, K. Effects of annealing on the structure formation in a thermotropic liquid crystalline copolyester. *Macromolecules* **1990**, *23*, 1035–1040.

17. Moniruzzaman, M.; Winey, K.I. Polymer nanocomposites containing carbon nanotubes. *Macromolecules* **2006**, *39*, 5194–5205.

18. Xie, X.L.; Mai, Y.W.; Zhou, X.P. Dispersion and alignment of carbon nanotubes in polymer matrix: A review. *Mater. Sci. Eng. R.* **2005**, *49*, 89–112.

19. Coleman, J.N.; Khan, U.; Blau, W.J.; Gun'ko, Y.K. Small but strong: A review of the mechanical properties of carbon nanotube-polymer composites. *Carbon* **2006**, *44*, 1624–1652.

20. Coleman, J.N.; Khan, U.; Gun'ko, Y.K. Mechanical reinforcement of polymers using carbon nanotubes. *Adv. Mater.* **2006**, *18*, 689–706.

21. Kiss, G. *In situ* composites: Blends of isotropic polymers and thermotropic liquid crystalline polymers. *Polym. Eng. Sci.* **1987**, *27*, 410–423.

22. Lin, Y.G.; Winter, H.H. High-temperature recrystallization and rheology of a thermotropic liquid crystalline polymer. *Macromolecules* **1991**, *24*, 2877–2882.

23. Kachidza, J.; Serpe, G.; Economy, J. Ordering processes in the 2,6-hydroxynaphthoic acid (HNA) rich copolyesters of p-hydroxybenzoic acid and HNA. *Makromol. Chem. Macromol. Symp.* **1992**, *53*, 65–75.

24. Cheng, H.K.F.; Sahoo, N.G.; Li, L.; Chan, S.H.; Zhao, J. Molecular interactions in PA6, LCP and their blend incorporated with functionalized carbon nanotubes. *Key Eng. Mater.* **2010**, *447–448*, 634–638.

25. Pracella, M.; Chiellini, E.; Dainelli, D. Blends of poly(tetrametylene terephthalate) with a liquid-crystalline polyester, poly(decamethylene 4,4'-terephthaloyldioxy-dibenzoate), 2. Crystallization kinetics and melting behavior. *Makromol. Chem.* **1989**, *190*, 175–184.

26. Saito, R.; Dresselhaus, D.; Dresselhaus, M.S. *Physical Properties of Carbon Nanotubes*; Imperial College Press: London, UK, 1998; p. 142.

27. Dresselhaus, M.S.; Lin, Y.M.; Rabin, O.; Jorio, A.; Souza Filho, A.G.; Pimenta, M.A.; Saito, R.; Samsonidze, G.G.; Dresselhaus, G. Nanowires and Nanotubes. *Mater. Sci. Eng. C* **2003**, *23*, 129–140.

28. Iijima, S.; Ichihashi, T. Single-shell carbon nanotubes of 1-nm diameter. *Nature* **1993**, *363*, 603–605.

29. Zhao, X.; Ohkohchi, M.; Wang, M.; Iijima, S.; Ichihashi, T.; Ando, Y. Preparation of high-grade carbon nanotubes by hydrogen arc discharge. *Carbon* **1997**, *35*, 775–782.

30. Quan, D.; Wagner, G.J.; Liu, W.K.; Yu, M.F.; Ruoff, R.S. Mechanics of carbon nanotubes. *Appl. Mech. Rev.* **2002**, *55*, 495–533.

31. Yakobson, B.I.; Avouris, P. Mechanical properties of carbon nanotubes. *Topics Appl. Phys.* **2001**, *80*, 287–327.

32. Reich, S.; Thomesn, C.; Maultzsch, J. *Carbon Nanotubes: Basic Concepts and Physical Properties*; Wiley-VCH: New York, NY, USA, 2004; p. 215.

33. Ajayan, P.M.; Schadler, L.S.; Graun, P.V. *Nanocomposite Science and Technology*; Wiley-VCH: Weinheim, Germany, 2003; p. 239.

34. Chae, H.G.; Liu, J.; Kumar, S. *Carbon Nanotubes Properties and Application*; O'Connell, M.J., Ed.; Taylor & Francis Group LLC: Boca Raton, FL, USA, 2006; Chapter 8, p. 213.

35. Lu, J.P. Elastic properties of carbon nanotubes and nanoropes. *Phys. Rev. Lett.* **1997**, *79*, 1297–1300.

36. Yu, M.F.; Lourie, O.; Dyer, M.J.; Moloni, K.; Kelly, T.F.; Ruoff, R.S. Strength and breaking mechanism of multiwalled carbon nanotubes under tensile load. *Science* **2000**, *287*, 637–640.

37. Sahoo, N.G.; Rana, S.; Cho, J.W.; Li, L.; Chan, S.H. Polymer nanocomposites based on functionalized carbon nanotubes. *Prog. Polym. Sci.* **2010**, *35*, 837–867.

38. Ma, P.C.; Siddiqui, N.A.; Marom, G.; Kim, J. Dispersion and functionalization of carbon nanotubes for polymer-based nanocomposites: A review. *Composites Part A* **2010**, *41*, 1345–1367.

39. Zhang, X.; Sreekumar, T.V.; Liu, T.; Kumar, S. Properties and structure of nitric acid oxidized single wall carbon nanotube films. *J. Phys. Chem. B* **2004**, *108*, 16435–16440.

40. Cho, J.W.; Kim, J.W.; Jung, Y.C.; Goo, N.S. Electroactive shape-memory polyurethane composites incorporating carbon nanotubes. *Macromol. Rapid. Commun.* **2005**, *26*, 412–416.

41. Georgakilas, V.; Kordatos, K.; Prato, M.; Guldi, D.M.; Holzingger, M.; Hirsch, A. Organic functionalization of carbon nanotubes. *J. Am. Chem. Soc.* **2002**, *124*, 760–761.

42. Zhang, Y.; Shi, Z.; Gu, Z.; Iijima, S. Structure modification of single-wall carbon nanotubes. *Carbon* **2000**, *38*, 2055–2059.

43. Datsyuk, V.; Kalyva, M.; Papagelis, K.; Parthenios, J.; Tasis, D.; Siokou, A.; Kallitsis, I.; Galiotis, C. Chemical oxidation of multiwalled carbon nanotubes. *Carbon* **2008**, *46*, 833–840.

44. Chen, J.; Rao, A.M.; Lyuksyutov, S.; Itkis, M.E.; Hamon, M.A.; Hu, H.; Cohn, R.W.; Eklund, P.C.; Colbert, D.T.; Smalley, R.E.; Haddon, R.C. Dissolution of full-length single-walled carbon nanotubes. *J. Phys. Chem. B* **2001**, *105*, 2525–2528.

45. Thess, A.; Lee, R.; Nikolaev, P.; Dai, H.; Petit, P.; Robert, J.; Xu, C.; Lee, Y.H.; Kim, S.G.; Rinzler, A.G.; *et al.* Crystalline ropes of metallic carbon nanotubes. *Science* **1996**, *273*, 483–487.

46. Mickelson, E.T.; Chiang, I.W.; Zimmerman, J.L.; Boul, P.J.; Lozano, J.; Liu, J.; Smalley, R.E.; Hauge, R.H.; Margrave, J.L. Solvation of fluorinated single-wall carbon nanotubes in alcohol solvents. *J. Phys. Chem. B* **1999**, *103*, 4318–4322.

47. Kelly, K.F.; Chiang, I.W.; Mickelson, E.T.; Hauge, R.H.; Margrave, J.L.; Wang, X.; Scuseria, G.E.; Radloff, C.; Halas, N.J. Insight into the mechanism of sidewall functionalization of single-walled nanotubes: An STM study. *Chem. Phys. Lett.* **1999**, *313*, 445–450.

48. Boul, P.J.; Liu, J.; Mickelson, E.T.; Huffman, C.B.; Ericson, L.M.; Chiang, I.W.; Smith, K.A.; Colbert, D.T.; Hauge, R.H.; Margrave, J.L.; *et al.* Reversible sidewall functionalization of buckytubes. *Chem. Phys. Lett.* **1999**, *310*, 367–372.

49. Cho, E.; Kim, H.; Kim, C.W.; Han, S. Ab initio study on the carbon nanotube with various degrees of functionalization. *Chem. Phys. Lett.* **2006**, *419*, 134–138.

50. Holzinger, M.; Steinmetz, J.; Samaille, D.; Glerup, M.; Paillet, M.; Bernier, P.; Ley, L.; Graupner, R. [2+1] cycloaddition for cross-linking SWCNTs. *Carbon* **2004**, *42*, 941–947.

51. Brunetti, F.G.; Herrero, M.A.; de Munoz, M.J.; Diaz-Ortiz, A.; Alfonsi, J.; Meneghetti, M.; Prato, M.; Vazquez, E. Microwave-induced multiple functionalization of carbon nanotubes. *J. Am. Chem. Soc.* **2008**, *130*, 8094–8100.

52. Sahoo, N.G.; Jung, Y.C.; Yue, H.J.; Cho, J.W. Effect of functionalized carbon nanotubes on molecular interaction and properties of polyurethane composites *Macromol. Chem. Phys.* **2006**, *207*, 1773–1780.

53. Sahoo, N.G.; Cheng, H.K.F.; Li, L.; Chan, S.H.; Judeh, Z.; Zhao, J. Specific functionalization of carbon nanotubes for advanced polymer nanocomposites. *Adv. Funct. Mater.* **2009**, *19*, 3962–3971.

54. Sahoo, N.G.; Cheng, H.K.F.; Pan, Y.; Li, L.; Chan, S.H.; Zhao, J. Strengthening of liquid crystalline polymer by functionalized carbon nanotubes through interfacial interaction and homogeneous dispersion. *Polym. Adv. Technol.* **2011**, *22*, 1452–1458.

55. Sahoo, N.G.; Cheng, H.K.F.; Bao, H.; Pan, Y.; Li, L.; Chan, S.H.; Zhao, J. Covalent functionalization of carbon nanotubes for ultimate intermolecular adhesion to liquid crystalline polymer. *Soft Matter* **2011**, *7*, 9505–9514.

56. Sahoo, N.G.; Cheng, H.K.F.; Bao, H.; Li, L.; Chan, S.H.; Zhao, J. Nitrophenyl functionalization of carbon nanotubes and its effect on properties of MWCNT/LCP composites. *Macromol. Res.* **2011**, *19*, 660–667.

57. Wu, X.; Chen, X.; Wang, J.; Liu, J.; Fan, Z.; Chen, X.; Chen, J. Functionalization of multiwalled carbon nanotubes with thermotropic liquid-crystalline polymer and thermal properties of composites. *Ind. Eng. Chem. Res.* **2011**, *50*, 891–897.

58. Wang, X.; Wang, J.; Zhao, W.; Zhang, L.; Zhong, X.; Li, R.; Ma, J. Synthesis and characterization of thermotropic liquid crystalline polyester/multi-walled carbon nanotube nanocomposites. *Appl. Surf. Sci.* **2010**, *256*, 1739–1743.

59. Lebovka, N.; Dadakova, T.; Lysetskiy, L.; Melezhyk, O.; Puchkovska, G.; Gavrilko, T.; Baran, J.; Drozd, M. Phase transitions, intermolecular interactions and electrical conductivity behavior in carbon multiwalled nanotubes/nematic liquid crystal composites. *J. Mol. Struct.* **2008**, *887*, 135–143.

60. Zhang, Q.; Fang, F.; Zhao, X.; Li, Y.; Zhu, M.; Chen, D. Use of dynamic rheological behavior to estimate the dispersion of carbon nanotubes in carbon nanotube/polymer composites. *J. Phys. Chem. B* **2008**, *112*, 12606–12611.

61. Baughman, R.H.; Zakhidov, A.A.; de Heer, W.A. Carbon nanotubes—The route toward applications. *Science* **2002**, *297*, 787–792.

62. Ericson, L.M.; Fan, H.; Peng, H.Q.; Davis, V.A.; Zhou, W.; Sulpizio, J.; Wang, Y.; Booker, R.; Vavro, J.; Guthy, C.; *et al.* Macroscopic, neat, single-walled carbon nanotube fibers. *Science* **2004**, *305*, 1447–1450.

63. Sreekumar, T.V.; Liu, T.; Kumar, S.; Ericson, L.M.; Hauge, R.H.; Smalley, R.E. Single-wall carbon nanotube films. *Chem. Mater.* **2003**, *15*, 175–178.

64. Sandler, J.K.W.; Kirk, J.E.; Kinloch, I.A.; Shaffer, M.S.P.; Windle, A.H. Ultra-low electrical percolation threshold in carbon-nanotube-epoxy composites. *Polymer* **2003**, *44*, 5893–5899.

65. Li, H.C.; Lu, S.Y.; Syue, S.H.; Hsu, W.K.; Chang, S.C. Conductivity enhancement of carbon nanotube composites by electrolyte addition. *Appl. Phys. Lett.* **2008**, *93*, 033104:1–033104:3.

66. Li, J.; Ma, P.C.; Chow, W.S.; To, C.K.; Tang, B.Z.; Kim, J.K. Correlations between percolation threshold, dispersion state, and aspect ratio of carbon nanotubes. *Adv. Funct. Mater.* **2007**, *17*, 3207–3215.

67. Du, F.; Fischer, J.E.; Winey, K.I. Coagulation method for preparing single-walled carbon nanotube/ poly (methyl methacrylate) composites and their modulus, electrical conductivity, and thermal stability. *J. Appl. Polym. Sci. B* **2003**, *41*, 3333–3338.

68. Bai, J.B.; Allaoui, A. Effect of the length and the aggregate size of MWNTs on the improvement efficiency of the mechanical and electrical properties of nanocomposites—Experimental investigation. *Compos. Part A* **2003**, *34*, 689–694.

69. Sahoo, N.G.; Cheng, H.K.F.; Cai, J.; Li, L.; Chan, S.H.; Zhao, J.; Yu, S. Improvement of mechanical and thermal properties of carbon nanotube composites through nanotube functionalization and processing methods. *Mater. Chem. Phys.* **2009**, *117*, 313–320.

70. Sahoo, N.G.; Thet, N.T.; Tan, Q.H.; Li, L.; Chan, S.H.; Zhao, J.; Yu, S. Effect of carbon nanotubes and processing methods on the properties of carbon nanotube/polypropylene composites. *J. Nanosci. Nanotechnol.* **2009**, *9*, 5910–5919.

71. Rasheed, A.; Chae, H.G.; Kumar, S.; Dadmun, M. Polymer nanotube nanocomposites: Correlating intermolecular interaction to ultimate properties. *Polymer* **2006**, *47*, 4734–4741.

72. Yu, A.; Hu, H.; Bekyarova, E.; Itkis, M.E.; Gao, J.; Zhao, B.; Haddon, R.C. Incorporation of highly dispersed single-walled carbon nanotubes in a polyimide matrix. *Compos. Sci. Technol.* **2006**, *66*, 1190–1197.

73. Chung, T.S. *Thermotropic Liquid Crystal Polymers: Thin-Film Polymerization, Characterization, BLENDS, and Applications*; CRC Press: London, UK, 2001; p. 364.

74. Roy, S.; Sahoo, N.G.; Das, C.K.; Li, L.; Chan, S.H. Improvement of properties of polyetherimide/liquid crystalline polymer blends in the presence of functionalized carbon nanotubes. *J. Nanosci. Nanotech.* **2009**, *9*, 1928–1934.

75. Tiwari, R.R.; Khilar, K.C.; Natarajan, U. New poly (phenylene oxide)/polystyrene blend nanocomposites with clay: Intercalation, thermal and mechanical properties. *J. Appl. Polym. Sci.* **2008**, *108*, 1818–1828.

76. Kalaitzidou, K.; Fukushima, H.; Miyagawa, H.; Drzal, L.T. Flexural and tensile moduli of polypropylene nanocomposites and comparison of experimental data to Halpin-Tsai and Tandon-Weng models. *Polym. Eng. Sci.* **2007**, *47*, 1796–1803.

77. Schaefer, D.W.; Justice, R.S. How nano are nanocomposites? *Macromolecules* **2007**, *40*, 8501–8517.

78. Halpin, J.C.; Kardos, J.L. The Halpin-Tsai equations: A review. *Polym. Eng. Sci.* **1976**, *16*, 344–352.

79. Agarwal, B.D.; Broutman, L.G. *Analysis and Performance of Fiber Composites*; Wiley: New York, NY, USA, 1980; p. 355.

80. Kim, J.Y. Carbon nanotube-reinforced thermotropic liquid crystal polymer nanocomposites. *Materials* **2009**, *2*, 1955–1974.

81. Incarnato, L.; Nobile, M.R.; Frigione, M.; Motta, O.; Acierno, D. Processing-structure-properties relationships in blends with thermotropic liquid crystalline polymers. *Intern. Polym. Process.* **1993**, *3*, 191–199.

82. Nobile, M.R.; Acierno, D.; Incarnato, L.; Amendola, E.; Nicolais, L.; Carfagna, C. Improvement of the processability of advanced polymers. *J. Appl. Polym. Sci.* **1990**, *41*, 2723–2737.

83. Cheng, H.K.F.; Sahoo, N.G.; Khin, T.H.; Li, L.; Chan, S.H.; Zhao, J.; Chen, G. The role of functionalized carbon nanotubes in a PA6/LCP blend. *J. Nanosci. Nanotech.* **2010**, *10*, 5242–5251.

84. Roy, S.; Sahoo, N.G.; Cheng, H.K.F.; Das, C.K.; Li, L.; Chan, S.H. Molecular interaction and properties of poly (ether ether ketone)/liquid crystalline polymer blends incorporated with functionalized carbon nanotubes. *J. Nanosci. Nanotech.* **2011**, *11*, 10408–10416.

85. Roy, S.; Sahoo, N.G.; Das, C.K.; Li, L.; Chan, S.H. Improvement of properties of PEI/LCP blends in the presence of functionalized carbon nanotubes. *J. Nanosci. Nanotech.* **2009**, *9*, 1928–1934.

86. Safadi, B.; Andrews, R.; Grulke, E.A. Multiwalled carbon nanotube polymer composites: Synthesis and characterization of thin films. *J. Appl. Polym. Sci.* **2002**, *84*, 2660–2669.

87. Jun'ichi, M.; John, M.T. Dispersion and major property enhancements in polymer/multiwall carbon nanotube nanocomposites via solid-state shear pulverization followed by melt mixing. *Macromolecules* **2008**, *41*, 5974–5977.

88. Volokhina, A.V.; Kudryavtsev, G.I. *Liquid-Crystal Polymers*; Plate, N.A., Ed.; Plenum Press: New York, NY, USA, 1992; chapter 10, p. 383.

89. Jou, W.S.; Cheng, H.Y.; Hsu, C.F. A carbon nanotube polymer-based composite with high electromagnetic shielding. *J. Electron. Mater.* **2006**, *35*, 462–470.

90. Chiu, J.C.; Chang, C.M.; Jou, W.S.; Cheng, W.H. High-performance Electromagnetic Susceptibility for a 2.5 Gb/s Plastic Transceiver Module Using Multi-Wall Carbon Nanotubes. In *Proceeding of the Electronic Components and Technology Conference*, San Diego, CA, USA, 30 May–2 June 2006; Institute of Electrical and Electronics Engineers (IEEE): New York, NY, USA, 2006; p. 183.